COMPUTING THE PITCH & ROLL EFFECTS ON DYNAMIC FORCES EXERTED ON PAVEMENTS BY HEAVY VEHICLES

Chiu Liu [1], Zhongren Wang[2], James N. Lee [3], and Xueyu Pang [4]

[1] Dept. of Civil & Environmental Engineering, Villanova University, 800 Lancaster Avenue, Villanova, PA 19085, Phone 610/519-4967, FAX 610/519-6754, uilcc3@yahoo.com

[2] Caltrans, Statewide Local Development Review, 1120 N Street MS-36 Sacramento, CA 95814, Phone 916/654-5672, FAX 916-653-3055, zhongren_wang@dot.ca.gov

[3] Caltrans, Division of Research and Innovations, 1101 R Street, Sacramento, CA 95814, Phone 916/324-2781, FAX 916-324-2669, james_n_lee@dot.ca.gov

[4] Dept. of Civil & Environmental Engineering, Villanova University, 800 Lancaster Avenue, Villanova, PA 19085, Phone 610/519-7932, FAX 610/519-6754, xueyu.pang@villanova.edu

ABSTRACT

Because varying the load distribution across a loading axle or in between two axles can change substantially the dynamic forces on both the front and rear wheels of a vehicle, a simple two-contact model is applied in this investigation to compute the effect of the vehicle load distribution on the dynamic forces exerted on pavement surfaces in terms of various physical parameters characterizing the vehicle-road interaction. The proposed model becomes an axle load model when placed perpendicular to a wheel path; and it can be a half of a vehicle model when placed along a wheel path. Dynamic responses of the models are computed in Excel worksheets in terms of the vehicle characteristics and the characteristics of road profiles. The intensities for both the rates of the dynamic forces and the dynamic forces are evaluated by considering the rotational effect induced by road profiles. It is demonstrated that the pitch & roll motion can change substantially the magnitudes of these dynamic quantities depending on weight distribution and vehicle characteristics. Practical scenarios are examined to illustrate the results obtained from this simple computational framework. The model may be applied to evaluate the dynamic forces exerted to pavement surfaces by the axle loads of vehicles or accelerated pavement-testing devices. Furthermore, it can be easily extended to assess damage caused by overweight vehicles and thus proper actions against the damage can be carried out.

KEY WORDS

Damage, dynamic force, dynamic loading coefficient, rate of dynamic forces, axle load, pavement, pitch, and roll.

INTRODUCTION

The vehicle-road interaction has been the subject of attentions in mechanistic-empirical pavement design (Ivey *et al* 1971; and Sousa *et al*, 1988). The vehicle dynamic forces exerted on pavement surfaces have been subjected to extensive investigations either by employing numerical methods (Lieh & Qi, 1995, Cebon 1999, and Gillespie et al 2000) or by deriving exact functional expressions (Liu 1997, and Liu et al 1998). Both the rates of dynamic forces (RDF) and the dynamic forces exerted on pavement surfaces were introduced to characterize pavement deterioration in connection with pavement ride quality (Liu 2000, and Liu 2001) and energy dissipation in pavements (Liu & Gazis, 1999). In order to take into account the pitch and/or the roll effects on dynamic forces exerted on pavement surfaces, a vehicle model with two wheel contacts is applied in this study. A set of equations associated with the model vehicle moving on road profiles is found by applying the spectral method and numerically solved in Excel worksheets. It is found that parameters of the model or vehicle types play important roles in the determination of the dynamic forces and the rate of dynamic forces RDF exerted on pavement surfaces.

FORMULATION

Shown in Figure 1 is a two-contact model is. The two contacts, separated by a distance l, are loaded with a sprung mass of M_s. The vertical coordinates for the center of sprung mass M_s, the unsprung mass M_1 on Contact 1, and the unsprung mass M_2 on Contact 2, are located at y_s, y_1, y_2 with respect to their equilibrium positions. The position of Contact 1 is given by $z(x_1)$ in the presence of a road profile $z(x)$, where the quantity x_1 is the horizontal coordinate of Contact 1. The position of Contact 2 is $z(x_2)$ if an axle model is assumed and is $z(x_1 + l)$ if a bicycle model is considered. Since the vehicle exhibits a rotational motion as it moves on an uneven road surface, a variable y_3 is introduced to characterize the rotation. The horizontal distance from the center of mass M_s to Contact 1 is parameterized as αl. When parameter α is equal to $1/2$, the distribution of the vehicle weight is symmetric about the centerline of the two contacts. If parameter α differs from $1/2$, the vehicle weight distribution is asymmetric.

We proceed to write down the dynamic equations governing the vertical oscillation for the a two-contact vehicle model

$$m_1 \ddot{y}_1 = F_2 - F_1 \tag{1}$$

$$m_2 \ddot{y}_2 = F_4 - F_3 \tag{2}$$

$$\beta M_s \ddot{y}_3 = (1-\alpha)F_3 - \alpha F_1 \tag{3}$$

$$M_s \ddot{y}_s = F_3 + F_1 \tag{4}$$

$$F_1 = -c_1(\dot{y}_s - \dot{y}_1 - \alpha\dot{y}_3) - k_1(y_s - y_1 - \alpha y_3) \tag{5a}$$

$$F_2 = -c_2(\dot{y}_1 - \dot{z}_1) - k_2(y_1 - z_1) \tag{5b}$$

$$F_3 = -c_3[\dot{y}_s - \dot{y}_2 + (1-\alpha)\dot{y}_3] - k_3[y_s - y_2 + (1-\alpha)y_3] \tag{5c}$$

$$F_4 = -c_4(\dot{y}_2 - \dot{z}_2) - k_4(y_2 - z_2) \tag{5d}$$

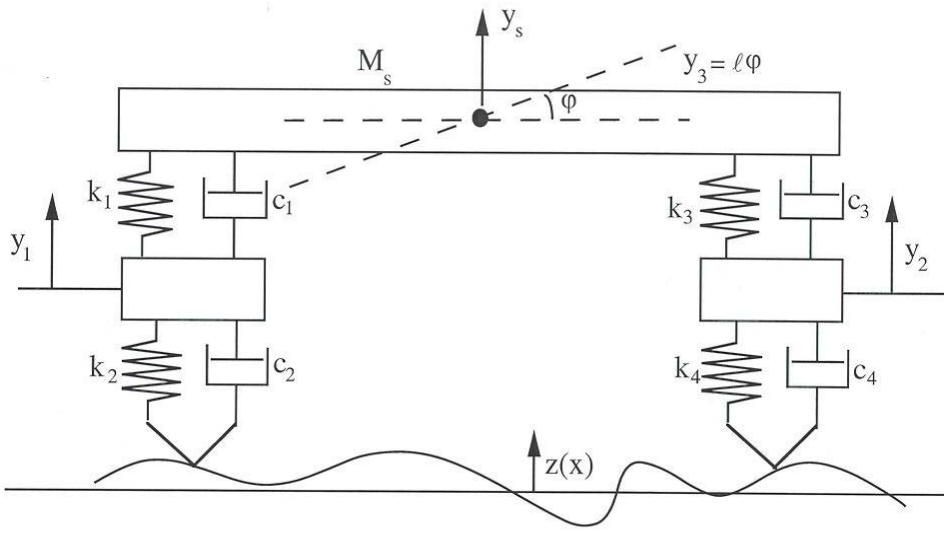

Figure 1: A simple two-contact vehicle model, which can be viewed either parrallel or perpendicular to travel direction.

Constants k_2 and k_4 characterize elastic property of tire at contact 1 and tire at contact 2. Constants k_1 and k_3 represent the elastic property of the suspension systems above tire contact 1 and contact 2, respectively. Each dashpot constant c_j combined with an elastic constant k_j (j=1–4) represents the visco-elasticity for a vehicle tire or a suspension system. Equation (3) describes the rotation in a vehicle, which can be the roll or the pitch motion depending on the relative positions of the two contacts. The parameter $\beta = \left(\frac{r_G}{l}\right)^2$, a dimensionless quantity, is the square of the ratio of the gyration distance and the separation of the contacts. For symmetric loading situation $0 \le \beta \le 1/4$; and for other loading situations $\beta \le 1/4$ usually holds unless a heavy wide load is present.

The dynamic tire forces exerted on the surface for a given excitation frequency ω at contacts 1 and 2, are found to be

$$F_{c1,\omega} = \mathrm{Re}\{\exp(i\omega t)[i\omega c_2 + k_2][A_{1\omega} - z_{1\omega}\exp(i\varsigma_{1\omega})]\} \quad \text{(Contact 1)} \qquad (6)$$

$$F_{c2,\omega} = \mathrm{Re}\{\exp(i\omega t)[i\omega c_4 + k_4][A_{2\omega} - z_{2\omega}\exp(i\varsigma_{2\omega})]\} \quad \text{(Contact 2)} \qquad (7)$$

The actual dynamic force for a given profile will be the summation of all the dynamic forces corresponding to different excitation frequencies, namely, $F_1(t) = \sum_n F_{c1,\omega_n}$ and $F_2(t) = \sum_n F_{c2,\omega_n}$. Equations (6-7) can be directly related to realistic models, e.g., the axle load model and the bicycle model.

Solving Eqs. (1)–(5) for a particular excitation frequency $\omega = \kappa v$, a product of the road profile spatial frequency κ and the vehicle speed v, the displacements $A_{1\omega}$ and $A_{2\omega}$ of the unsprung mass m_1 and m_2 can be found, respectively;

$$A_{1\omega} = D_{\omega}^{-1}\left[z_{1\omega}(k_2 + i\omega c_2)\psi_{1\omega}\exp(i\varsigma_{1\omega}) + z_{2\omega}(k_4 + i\omega c_4)\psi_{2\omega}\exp(i\varsigma_{2\omega})\right] \quad (8a)$$

$$A_{2\omega} = D_{\omega}^{-1}\left[z_{1\omega}(k_2 + i\omega c_2)\varphi_{1\omega}\exp(i\varsigma_{1\omega}) + z_{2\omega}(k_4 + i\omega c_4)\varphi_{2\omega}\exp(i\varsigma_{2\omega})\right] \quad (8b)$$

where the quantities $\varsigma_{1\omega}$ ($z_{1\omega}$) and $\varsigma_{2\omega}$ ($z_{2\omega}$) are the phase angles (profile amplitudes) for contact 1 and contact 2, respectively; and

$$D_{\omega} = (i\omega c_1 + k_1)(i\omega c_3 + k_3)(i\omega c_2 + k_2 - m_1\omega^2)(i\omega c_4 + k_4 - m_2\omega^2) - \beta M_s\omega^2(G_{1\omega} + G_{2\omega} - G_{3\omega}) - M_s\omega^2[\alpha^2 G_{1\omega} + (1-\alpha)^2 G_{2\omega}] \quad (8c)$$

$$\psi_{1\omega} = (i\omega c_1 + k_1)(i\omega c_3 + k_3)(i\omega c_4 + k_4 - m_2\omega^2) - \beta M_s\omega^2 \times (H_{1\omega} + H_{2\omega} + H_{3\omega} - H_{4\omega}) - M_s\omega^2[\alpha^2(H_{1\omega} + H_{3\omega}) + (1-\alpha)^2 H_{2\omega}] \quad (8d)$$

$$\psi_{2\omega} = [\alpha(1-\alpha) - \beta]M_s\omega^2(i\omega c_1 + k_1)(i\omega c_3 + k_3) \quad (8e)$$

$$\varphi_{2\omega} = (i\omega c_1 + k_1)(i\omega c_3 + k_3)(i\omega c_2 + k_2 - m_1\omega^2) - \beta M_s\omega^2 \times (L_{1\omega} + L_{2\omega} + L_{3\omega} - L_{4\omega}) - M_s\omega^2[(1-\alpha)^2(L_{1\omega} + L_{3\omega}) + \alpha^2 L_{2\omega}] \quad (8f)$$

$$\varphi_{1\omega} = \psi_{2\omega} \quad (8g)$$

where

$$G_{1\omega} = (i\omega c_1 + k_1)(i\omega c_2 + k_2 - m_1\omega^2)(i\omega c_3 + k_3 + i\omega c_4 + k_4 - m_2\omega^2)$$

$$G_{2\omega} = (i\omega c_3 + k_3)(i\omega c_4 + k_4 - m_2\omega^2)(i\omega c_1 + k_1 + i\omega c_2 + k_2 - m_1\omega^2)$$

$$G_{3\omega} = M_s\omega^2(i\omega c_1 + k_1 + i\omega c_2 + k_2 - m_1\omega^2)(i\omega c_3 + k_3 + i\omega c_4 + k_4 - m_2\omega^2)$$

$$H_{1\omega} = (i\omega c_1 + k_1)(i\omega c_4 + k_4 - m_2\omega^2)$$

$$H_{2\omega} = (i\omega c_3 + k_3)(i\omega c_4 + k_4 - m_2\omega^2)$$

$$H_{3\omega} = (i\omega c_1 + k_1)(i\omega c_3 + k_3)$$

$$H_{4\omega} = M_s\omega^2(i\omega c_3 + k_3 + i\omega c_4 + k_4 - m_2\omega^2)$$

$$L_{1\omega} = (i\omega c_3 + k_3)(i\omega c_2 + k_2 - m_1\omega^2)$$

$$L_{2\omega} = (i\omega c_1 + k_1)(i\omega c_2 + k_2 - m_1\omega^2),$$

$$L_{3\omega} = H_{3\omega}$$

$$L_{4\omega} = M_s\omega^2(i\omega c_1 + k_1 + i\omega c_2 + k_2 - m_1\omega^2).$$

The second term in the right hand side of Equations (8c-8f) represent the rotational (or roll) effect of the axle loading.

AXLE LOAD MODEL

In practices, truckloads to pavements may be decomposed to several axle loads (AASHTO 93). Using the proposed model, Contact 1 and 2 represent the tire contacts in the left and the right wheel path within a traffic lane, respectively. If the axle load is usually symmetric, implying that

$$\alpha = 1/2;\ k_1 = k_3;\ k_2 = k_4;\ c_1 = c_3;\ c_2 = c_4 \quad (9)$$

One may derive the following expressions using Eqs (1-7):

$$\psi_{1\omega} = \varphi_{2\omega} = \left(i\omega c_1 + k_1 - m_s\omega^2\right)\left(X - 4\beta Y\right) - \psi_{2\omega} \tag{10}$$

$$\psi_{2\omega} = \varphi_{1\omega} = \frac{1-4\beta}{2}\left(i\omega c_1 + k_1\right)^2; \quad D_\omega = (X-Y)(X-4\beta Y) \tag{11}$$

$$X = \left(i\omega c_1 + k_1\right)\left(i\omega c_2 + k_2 - m_1\omega^2\right)$$

$$Y = m_s\omega^2\left(i\omega c_1 + k_1 + i\omega c_2 + k_2 - m_1\omega^2\right)$$

where the quantity $m_s = M_s / 2$. It can be inferred from Eqs. (6-7) and (9) that if both wheel path profiles in a lane is exactly the same, there is no rotation (roll) effect present in the axle load system because the vibrations on both contacts are synchronized. This agrees with our intuition. The rotational moment of inertia characterized by parameter β varies as the weight distribution within a vehicle changes.

In a wide load situation, the parameter β could be greater than 0.25. When the sprung mass is distributed uniformly across the width of the vehicle, the quantity β is found to be 1/12. When the sprung mass is concentrated at the center of mass, the quantity β approaches a small number close to 0, in which the roll effect is most severe if present. When the sprung mass is split into two halves of equal weight placing above the two contacts respectively, the quantity β takes the value of $1/4$; and under this condition, the axle load model is split to two equivalent quarter vehicle models (Liu et al, 1998). It is a mistake to think that the roll effect is not present in a quarter-vehicle model. In other words, when parameter β is close to $1/4$, it is legitimate to represent a vehicle by a quarter-vehicle model. Employing Eqs (6-9), we express the dynamic force exerted on the left wheel path (LWP) (Contact 1) on a pavement surface, as

$$F_{c1,\omega} = \left(z_{2\omega} - z_{1\omega}\right)\frac{\left(i\omega c_2 + k_2\right)^2}{D_\omega}\psi_{2\omega}e^{i\omega t} + H_{c1,\omega} \tag{12}$$

$$H_{c1,\omega} = z_{1\omega}\left(i\omega c_2 + k_2\right)^2\left(\frac{i\omega c_1 + k_1 - m_s\omega^2}{X - Y} - 1\right)e^{i\omega t} \tag{13}$$

One can work out similar expressions for contact 2, namely, for the right wheel path (RWP). The first term in Equation (12) vanishes if the LWP is perfectly correlated with the RWP. When the correlation between the two wheel paths is high, the first term in the RHS of Eq. (12) can be much smaller than the second term in the RHS of the equation, indicating that Eq. (12) coincides with the dynamic force computed via a quarter vehicle model. Under such conditions, the standard deviation of the rate of dynamic forces S_{J_t} and the standard deviation of the dynamic loading forces DLC (Liu et al 1998, and Gillespie et al, 2000) are approximated by

$$DLC(\beta) \approx DLC(1/4) \tag{14}$$

$$S_{J_t}(\beta) \approx S_{J_t}(1/4) \tag{15}$$

Both quantities DLC and S_{J_t} are computed by inputting profile data to an Excel sheet using and assuming a vehcle is traveling at 80 km/hr (50 mph). Three road profiles, OH8310, OH 8314, and OH8316, collected in a NCHRP project (Janoff et al 1983) are used

in the computation. The ride quality rating for road sections OH8310, OH 8314, and OH8316 are respectively 3.8, 2.3, 1.3. By selecting the ratio of the sprung and the unsprung mass $m_1 / m_s = 0.2$, the dashpot constant $c_1 / m_s = 1.86$, the elastic constant for the suspension system $k_1 / m_s = 146$, the tire spring constant $k_2 / m_s = 1028$, the visco–damping characteristics of the tire $c_2 / m_s = 0.15$, and the sum of the sprung and the unsprung mass $m_1 + m_s = 4086$ kg (half of 18 kips), we plot both quantities *DLC* and S_{J_t} in Figs. 2 and 3, respectively. It can be inferred from the figures that the roll effect becomes less important when β moves away from the origin; and when parameter β approaches the origin, the roll effect becomes strong because a small differentiation between the LWP and the RWP easily excite the vehicle. In addition, by examining Figs. 2 and 3, one finds that the effect is more pronounced when the pavement ride quality is low or its profile gets rougher.

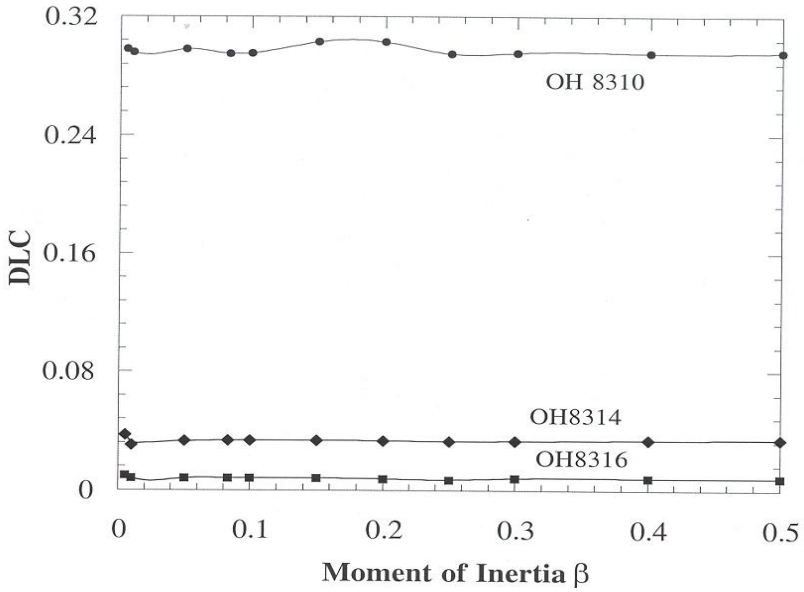

Figure 2: The dynamic loading coefficient (DLC) evaluated using 3 different road profiles is plotted against the normalized moment of inertia β.

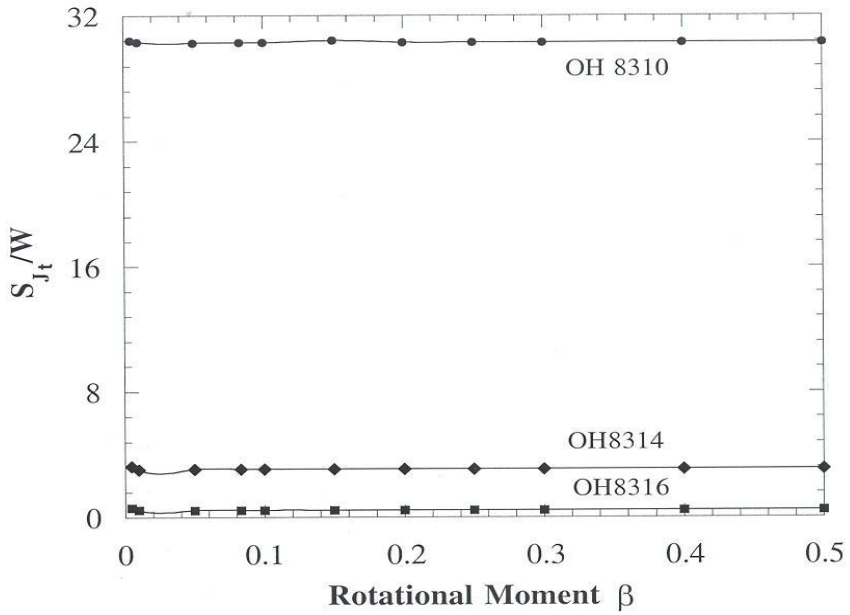

Figure 3: The standard deviation of the rate of dyanmic force (S_{J_t}) evaluated using 3 road profiles, is plotted against the normalized moment of inertia β.

BICYCLE MODEL

Let us assume that both the front axle and the rear axle possess the same mechanical characteristics and the loads are distributed symmetrically about the midpoint between the two axles. Employing Eqs (9–11), we express the dynamic forces exerted on a pavement surface by the front wheel (the path for contact 1) as

$$F_{c1,\omega} = z_{1\omega} \frac{(i\omega c_2 + k_2)^2}{D_\omega} \left(e^{-i\omega \ell / v} - 1\right) e^{i\omega t} \psi_{2\omega} + H_{c1,\omega} \tag{16}$$

$$H_{c1,\omega} = z_{1\omega} (i\omega c_2 + k_2)^2 e^{i\omega t} \left(\frac{i\omega c_1 + k_1 - m_s \omega^2}{X - Y} - 1 \right) \tag{17}$$

The front wheel becomes the rear wheel by switching the moving direction, and vise versa. Similar expressions for contact 2 can be obtained. The first term in Equation (16) vanishes if the distance l between the two wheels disappears. The expression for the dynamic forces due to each contact is reduced to the expression corresponding to a half of an axle load. The first term in the RHS of Eq. (16) produces a small correction to the second term in the RHS of the equation. Under such conditions, Equations (14) and (15) still hold for the half of a vehicle model so long as the load isn't concentrated in the middle of the two contacts.

Next, we compute the dynamic forces using road profile OH8310 and by keeping the same parameter values set for the previous section. It can be seen from both Fig. 4 and Fig. 5 that the rotation (pitch) effect has some influence in both quantities DLC and S_{J_t}. The rotation (pitch) effect becomes apparent when the rotational moment of inertia is small, e.g., when parameter β is close to zero, say 0.01, corresponding to a situation in which the load

is concentrated in the middle. Such a small parameter β should be avoided in practices by distributing the uniformly more or less uniformly within a vehicle. When the load distribution is uniform, parameters β is in the neighborhood of $1/12$. The horizontal line in both Figures 4 and 5 represent the results obtained from the quarter vehicle model. The large oscillation of the quantity DLC reflects the fact that the spectral density for profile OH8310 peaks at the wavelength of about 7 meters. Comparing Fig. 2 and Fig.4, one notice that the pitch effect is more pronounced than the roll effect for a moving load because of the random fluctuation of a wheel path profile.

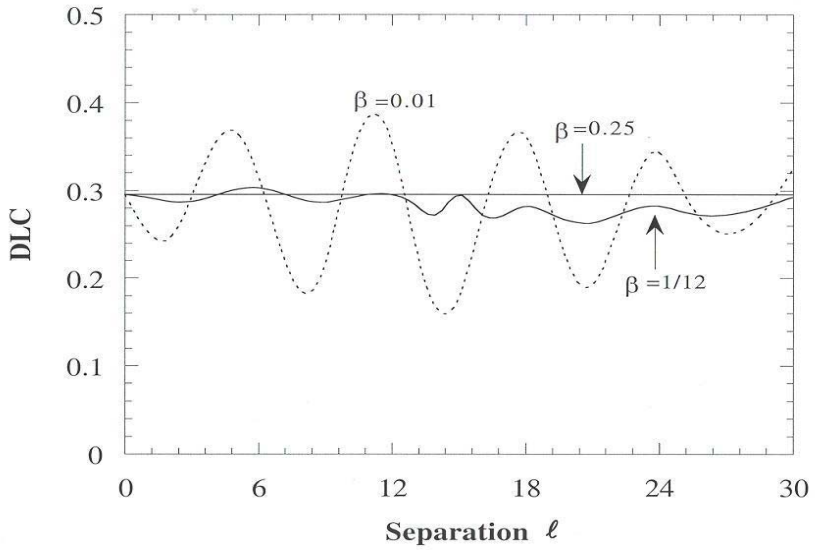

Figure 4: The dynamic loading coefficient (DLC) evaluated using road profile OH8310, is plotted against the separation ℓ between the two contacts.

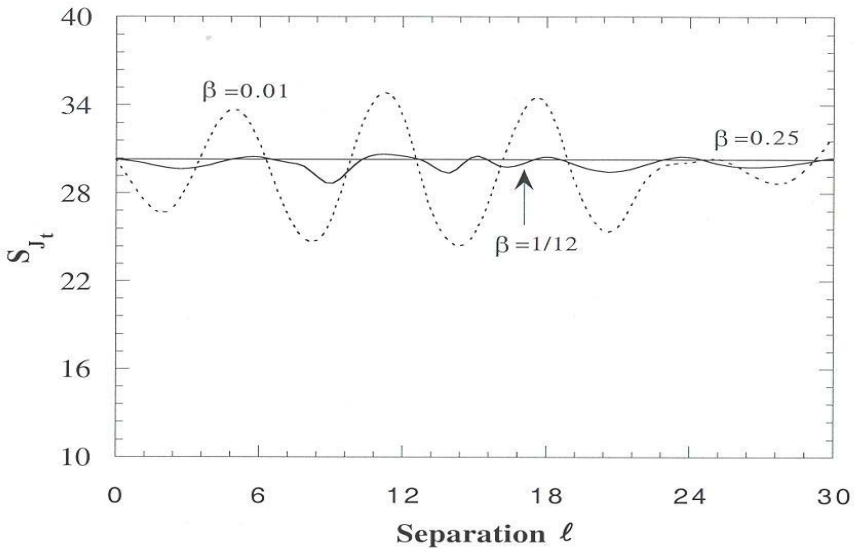

Figure 5: The standard deviation of the rate of dynamic force (S_{J_t}) evaluated using road profile OH8310, is plotted against the separation ℓ between the two contacts.

SUMMARY AND CONCLUSION

Both the pitch and roll effects on the dynamic forces exerted on pavement surfaces by a moving load have been examined by exactly solving a set of dynamic equations for a two–contact model. Analytic expressions for the dynamic forces, the DLC, and the RDF are derived. The intensity of the RDF and the DLC are computed by inputting into Excel worksheets real road profiles of different ride quality. The standard deviation of the RDF and the DLC are derived by taking into account the rotation effect on an uneven road. It is found that

- Both the DLC and the RDF becomes strong when the weight distribution is concentrated within a vehicle, namely, when parameter β is in the neighborhood of the origin.
- Both the DLC and the RDF are quite stable when the moment of inertia is away from the origin, namely when $\beta \geq 0.03$ according to the numerical results. This justifies the using of the quarter vehicle model for calculating the statistical quantities such as DLC or RDF concerning dynamic forces exerted on pavement surfaces.
- In order to decrease dynamic loads on pavements, the total load on a vehicle should be spreaded out as uniform as possible by increasing the moment parameter β.

The model can be used for other purposes:

- Study the weight effect on pavement dynamic response.
- Investigate the unsymmetrical loading effect on dynamic forces by tuning the parameter α.
- Estimate to the magnitude of the pitch and roll motion in heavy vehicles.
- Relate to either a tandem or a single axle load applied to a road test section using accelerated pavement testing devices if the test section profile can be accurately measured (Groenendijk, 1997; Hugo, 1996; and Pidwerbesky, 1995).

REFERENCES

Cebon, D. (1999). Handbook Of Vehicle-Road Interaction, Swets en Zeitlinger, Netherlands

Gillespie, T. D., Karamihas, M. S., (2000). "Simplified Models For Truck Dynamic Response To Road Inputs," Int. J. Vehicle Design, 7 (2), 231-247

Groenendijk, J., Volgelzang, C. H., Miradi, A., Molenaar, A. A. A., and Dohmen, L. J. M. (1997). "Rutting Development in Linear Tracking Test Pavements to Evaluate Shell Subgrade Strain Criterion," Transp. Res. Rec. 1570, 23-29, TRB, NRC, Washington D. C.

Hugo, F. (1996). "Executive Summary Report on the Production of the Prototype Texas Mobile Load Simulator," Center for Transp. Res. Report 1978-2F, Bureau of Engineer Research, The University of Texas at Austin

Ivey, D. L., Keese, C. J., Neill, A. H., and Brenner, C (1971). "Interaction of Vehicle And Road Surface," Highway Research Record

M. S. Janoff, J. B. Nick, P. S. Davit, and G. F. Hayhoe (1985). "Pavement Roughness and Rideability," NCHRP Report 275, TRB, NRC, Washington D. C.

Lieh, J., and Qi, W. (1995), "Simulation Of Dynamic Truck Loading On Pavements Using Measured Road Roughness," Transp. Res. Rec. 1501, 13-21, TRB, NRC.

Liu, C. (2000). "Vehicle–Road Interaction, Evolution of Road Profiles and Present Serviceability Index," Int. J. Road Materials and Pavement Design, Vol. 1, 2000, 35-51

Liu, C. (2001). "Pavement Repsonse to Moving Loads," International Journal of Road Materials and Pavement Design, 2 (3), pp 263-282.

Liu, C., and Gazis, D. (1998). "Surface Roughness Effect on the Dynamic Response of Pavement Structure," Transp. Res. Rec. 1643, 14-19, TRB, NRC, Washington D.C.

Liu, C., McCullough, B. F., and Herman, R. (1998). "Pavement Deterioration, Rate of Dynamic Force, And Ride Quality," Transp. Res. Rec. 1643, 14-19, TRB, NRC, Washington D.C.

Pidwerbesky, B. D. (1995). "Accelerated Dynamic loading of the Flexible Pavements At the Canterbury Accelerated Pavement Testing Indoor Facilities," Transp. Res. Rec., vol. 1482, 79-86, TRB, NRC, Washington D. C.

Sayers, M. W., and Karamihas, M. S., (1996). Interpretation Of Road Roughness Profile Data, Final Report, FHWA-RD-96-101

Sousa, J. B, Lymer, J., Chen, S. S., and Monismith, C. L. (1988). "Effect of Dynamic Loads on Performance of Asphalt Concrete Pavements," Transp. Res. Record, Vol. 1207, 145-168.